NACA

RESEARCH MEMORANDUM

SOME EXPERIMENTS ON THE FLUTTER OF WINGS WITH SWEEPBACK IN THE TRANSONIC SPEED RANGE UTILIZING ROCKET-PROPELLED VEHICLES

By William T. Lauten, Jr. and J. M. Teitelbaum

Langley Aeronautical Laboratory
Langley Air Force Base, Va.

NATIONAL ADVISORY COMMITTEE
FOR AERONAUTICS
WASHINGTON

May 18, 1950
Declassified April 15, 1958

NATIONAL ADVISORY COMMITTEE FOR AERONAUTICS

RESEARCH MEMORANDUM

SOME EXPERIMENTS ON THE FLUTTER OF WINGS WITH SWEEPBACK IN THE TRANSONIC SPEED RANGE UTILIZING ROCKET-PROPELLED VEHICLES

By William T. Lauten, Jr. and J. M. Teitelbaum

SUMMARY

As a continuation of an investigation of flutter in the transonic speed range, nine pairs of wings of various angles of sweepback and aspect ratios have been tested using rocket-propelled vehicles, and the results are presented herein. The primary objective of these experiments was to obtain systematic data concerning the effect of sweepback on flutter in the transonic and low-supersonic speed ranges.

In one series of experiments the wings tested had constant length-to-chord ratios, constant stiffnesses, and varying sweep angles. The unswept-wing configuration of this series failed in a low-frequency flutter mode which was apparently a combination of wing bending and body pitch. The 30° sweptback wings of this series fluttered at a Mach number of 0.78 in a wing bending-torsion flutter mode. Similar wings with 45° and 60° sweepback did not flutter up to the highest Mach number of the tests (approx. 1.45). In another series of tests on wings of constant aspect ratio the unswept and the 30° sweptback wings diverged and the 60° sweptback wings fluttered at a Mach number 1.01. In addition to these experiments, two other unrelated tests were performed. In the first of these tests the wings diverged and failed at a speed that was lower than the values calculated from various divergence theories. In the second test the wings failed in the low-frequency flutter mode mentioned previously.

A comparison of the experimental flutter speeds with the subsonic flutter theory, which assumes two-dimensional, incompressible flow and includes sweepback and mode shape, but not body-freedom modes, shows the theory to be conservative, particularly above $M = 0.9$.

INTRODUCTION

The problem of flutter in the transonic speed range is becoming increasingly important. Since very few experimental data have been reported for this region and a general theory describing transonic flutter phenomena is not available at the present time, the National Advisory Committee for Aeronautics, as a part of a general investigation of flutter, is conducting flutter experiments in the transonic speed range using rocket-propelled vehicles.

Previous flutter experiments employing rocket vehicles are reported in references 1 to 4. The initial test using this method, reported in reference 1, was primarily a test to determine the feasibility of the rocket technique. It employed a simplified breakwire system of instrumentation and a low-acceleration (4g) rocket vehicle having a maximum Mach number of approximately 1.1. The wings tested were swept back and served as horizontal stabilizing tail fins. The results indicated that more comprehensive instrumentation would be desirable. Consequently, another experiment, employing a similar configuration and instrumented to detect wing vibrations, was performed and is reported in reference 2. Since these two tests indicated that the rocket vehicle was a satisfactory means of obtaining flutter data in the desired speed range, the investigation was continued using this method. Reference 3 reports two tests of unswept wings utilizing this technique. The first of these two tests resulted in conventional bending-torsion flutter at a transonic Mach number, but the second test resulted in an unexpected low-frequency flutter in a mode which was apparently a combination of wing bending and body pitching.

In order to extend the investigation into the low-supersonic speed range a high-acceleration vehicle (52g), having a maximum Mach number of approximately 1.6, was employed. The results of these experiments, which were intended to explore the usefulness of the high-acceleration vehicle, are reported in reference 4. The test wings, instead of being used as tail fins as on the low-acceleration rocket, were placed slightly behind the center of gravity of the entire model and the vehicle was stabilized with small tail fins. These tests indicated that the high-acceleration vehicle was also a satisfactory means of obtaining flutter information. The experiments reported herein are a continuation of the work of reference 4 and employed a similar vehicle which had an acceleration of approximately 16g and a maximum Mach number of approximately 1.5.

The primary objective of the experiments reported in this paper was to obtain systematic data concerning the effect of sweep on flutter in the transonic and low-supersonic speed ranges. To obtain this information one group of four pairs of wings and one group of three pairs of wings were designed. It was intended that the first group should yield

information concerning the effect of sweep on flutter while maintaining constant the wing stiffnesses and the length-to-chord ratio. The second group was designed with the intention of investigating the effect of sweep while maintaining a constant aspect ratio.

In addition to these tests two other unrelated tests were performed. One pair of wings was designed with the center of gravity far rearward in an attempt to obtain supersonic flutter with an unswept wing. The second pair, which was similar to those that failed in the low-frequency flutter mode mentioned previously, was tested to determine what effect radical changes in the over-all configuration would have on this low-frequency flutter.

SYMBOLS

c	wing chord measured perpendicular to leading edge, inches
l	length of wing measured along leading edge, inches
Λ	angle of sweepback, degrees
x_o	distance of elastic axis behind leading edge measured perpendicular to leading edge when wing is mounted in block as flown, percent chord
x_1	distance of center of gravity of wing section behind leading edge measured perpendicular to leading edge, percent chord
a	nondimensional elastic-axis position $\left(\frac{2x_o}{100} - 1\right)$
$a + x_\alpha$	nondimensional center-of-gravity position $\left(\frac{2x_1}{100} - 1\right)$
x_α	nondimensional difference between center-of-gravity and elastic-axis positions $(a + x_\alpha - a)$
M	Mach number
M_{cr}	theoretical Mach number at which sonic velocity is first attained over section of wing at zero lift
A	aspect ratio (including fuselage area between wing roots) $\left(\frac{\text{Span}^2}{\text{Wing area}}\right)$

A_g	geometric aspect ratio of one wing panel $\left(\frac{l \cos^2 \Lambda}{c}\right)$
b	semichord of wing measured perpendicular to leading edge, feet
c.g.	center of gravity of entire missile, inches from nose
L.E.	position of leading edge of wing at root, inches from nose
ρ	air density, slugs per cubic foot
m	mass of wing per unit length, slugs per foot
κ	ratio of mass of cylinder of testing medium of diameter equal to chord of wing to mass of wing, both taken for an equal length of span $(\pi\rho b^2/m)$
I_α	polar moment of inertia about elastic axis, slug-feet^2 per foot
r_α^2	square of nondimensional radius of gyration about elastic axis (I_α/mb^2)
f_{h_1}	first bending natural frequency, cycles per second
f_{h_2}	second bending natural frequency, cycles per second
f_t	first torsion natural frequency, cycles per second
f_α	uncoupled first torsion frequency relative to elastic axis, cycles per second
ω_α	torsional frequency, radians per second $(2\pi f_\alpha)$
g_{h_1}	structural damping coefficient in first bending
g_α	structural damping coefficient in torsion
GJ	torsional rigidity, pound-inches^2
EI	bending rigidity, pound-inches^2
g	acceleration due to gravity, 32.2 feet per second^2
p_s	static pressure, pounds per foot^2

T	free-air temperature, ^{o}F absolute
q	dynamic pressure, pounds per $foot^2$
v_c	velocity of sound in air, feet per second
v_e	experimental flutter speed, feet per second
f_{f_e}	experimental flutter frequency, cycles per second
v_m	experimental speed (maximum or break), feet per second
v_R	reference wing flutter speed (free stream) based on theory of reference 5, feet per second
f_R	reference wing flutter frequency based on theory of reference 5, cycles per second
v_D	reference wing divergence speed based on theory of reference 6, feet per second
$1/k$	reduced wave length $\left(\frac{v_R \cos \Lambda}{2\pi b f_R}\right)$

MODELS AND INSTRUMENTATION

Rocket Vehicles

The rocket vehicles used in these tests were basically the same as those reported in reference 4, except that in the tests reported herein a rocket motor producing 1200 pounds of thrust for approximately 3 seconds replaced the type formerly used, thereby reducing the longitudinal acceleration from a maximum of approximately 52g to a maximum of 16g. The models weighed approximately 55 pounds without the propelling charge and approximately 81 pounds with the propelling charge in place. The corresponding moments of inertia in pitch about the center-of-gravity position were approximately 4.3 and 5.2 slug-feet squared. Photographs of representative models on the launching rack are shown in figure 1. A sketch of the test vehicle is shown in figure 2.

Flutter Wings

The flutter wings were so attached to the test vehicle that the mean aerodynamic center of the test wings was either at or slightly behind the center of gravity of the model without the propelling charge. The center

of gravity without the propelling charge was approximately 0.5 inch behind the center of gravity with the propelling charge in place. The center of gravity of each model without the propellant and the position on the model of each pair of wings is listed in table I. The wing characteristics which were used in the calculation of flutter and divergence speeds based on theoretical work were determined from preflight structural and vibration tests and are also given in table I. Sketches of the various wing configurations tested are shown in figures 3, 4, and 5.

The test program reported herein was divided into three groups. The first group consisted of two pairs of wings (models 5 and 6) designed for two unrelated tests. The first pair was designed with the center of gravity far rearward in an attempt to obtain supersonic flutter with an unswept wing and thus possibly to serve as a check on the tests performed in the Langley supersonic flutter apparatus and reported in reference 7. The wings had a circular-arc, 9-percent-thick airfoil section, were constructed of chordwise laminated white pine with steel inserts, and had a trailing edge formed of a bismuth-tin alloy. The second pair of wings (model 6), having an NACA 65A006 airfoil section constructed of white pine with surface inserts of aluminum alloy, were so built to have the same low bending-torsion frequency ratio of the wings tested on the low-acceleration rocket (reference 3).

The second group (models 7, 8, 9, and 10), consisting of four pairs of wings, was designed to investigate the effect on flutter speed of varying the degree of sweepback while maintaining constant the length-to-chord ratios and the structural stiffnesses of the wings. These wings were constructed of maple laminated spanwise and had an NACA 65A009 section taken perpendicular to the leading edge. Although the wings were identical in construction, the fact that they were swept necessitated skewed root attachment blocks which resulted in an increase (noted in table I) in the bending and torsional frequencies and in a shift in the elastic axis toward the trailing edge. For this series of tests model 7 had 0° sweep; model 8, 30° sweep; model 9, 45° sweep; and model 10, 60° sweep.

The last group of tests was composed of three pairs of wings which were unswept (model 11), swept back 30° (model 12), and swept back 60° (model 13) in an attempt to determine the effect of sweepback on the flutter speed while maintaining a constant aspect ratio. These wings were constructed of spruce laminated in thickness resulting in a three-ply wing. The grain of the wood on the upper and lower surfaces was run spanwise for bending strength and the grain of the center lamination was run parallel to the air stream to increase the strength of the leading and trailing edges. These wings had an NACA 65A005 section parallel to the air stream. This design resulted in wings having approximately constant torsional frequencies and decreasing bending frequencies with increase in sweep angle.

Telemeters and Strain Gages

Each model was equipped with a two-channel telemeter housed in the metal nose and designed to transmit the wing frequencies detected by strain gages located near the root of the wings. These strain gages were mounted on the wings to detect wing torsion, with the exception of model 6, which had the strain gages mounted to detect wing bending. The transmitted signals from the telemeter, which was provided by the Langley Instrument Research Division, were recorded at two receiving stations near the launching area. Accurate wing frequencies could be determined from the records but no effort was made to evaluate the magnitude of the flutter oscillation because the response of the recording system decreased with increase in frequency. During the flight tests the models were tracked with continuous-wave radar in order that the flight velocity could be determined. Timing signals were simultaneously fed to both the continuous-wave radar and the telemeter recorder in order that the data could be correlated.

RESULTS AND DISCUSSION

In general, take-off and the power-on flight of the models were smooth up until wing failure. The failure of one wing of a model caused the model to assume a helical flight path and the information obtained concerning the remaining wing after this time could no longer be considered for a flutter analysis. In these cases no velocity data are recorded in table II for the wing that did not fail.

Prior to flight testing, preliminary flutter and divergence speeds were calculated by using standard air density in the approximate formulas given in reference 8. After flight testing, the reference flutter and divergence speeds were calculated by theories which are more specific than that used in the preliminary calculations and the air density employed in these calculations was that determined at the time of flight. Reference flutter speeds were calculated from the theory of reference 5 which employs two-dimensional incompressible flow, includes sweepback, uses the uncoupled first bending and first torsional frequencies and, associated with these frequencies, assumes the mode shape of a uniform cantilever beam clamped perpendicular to its length. A re-examination of the data with the inclusion of missile free-body modes in the calculation of flutter speeds would be desirable but is beyond the scope of the present paper. The reference divergence speeds were calculated from the theory of reference 6 which includes the effect of sweep and makes corrections for the effect of aspect ratio and compressibility.

In preceding papers on transonic flutter (references 1 to 4, 7, and 9 to 11) the experimental flutter speeds have been compared with reference flutter speeds derived from the theory of reference 8. Since reference 8 does not treat the effect of sweep, it is thought that reference 5 is more appropriate for the purpose of this paper. This statement should be remembered when the results of this paper are compared with data published in previous papers. It may be noted, however, that for the straight wings reported herein, calculations were made to check the numerical differences resulting from the use of the two methods (references 5 and 8). In these calculations the values obtained from the theory of reference 5 ranged between 0.4 and 3.6 percent higher and averaged 2 percent higher than the values obtained from reference 8.

Model 5

The test of model 5 was conducted to determine the effect on flutter of an extremely rearward wing center-of-gravity position. For these particular wings the center-of-gravity and elastic-axis positions were very near each other with the center of gravity located behind the elastic axis as noted in table I. It was thought from the preliminary calculations that the flutter speed would be reached before the divergence speed. However, the record reproduced in figure 6(a) clearly shows that wing divergence did occur. Divergence-speed calculations were made for this model from various theories but all values obtained exceeded the experimental failure speed by at least 200 feet per second. No conclusions are drawn as to the reason for wing divergence. There is a possibility, however, of a forward shift in the center of pressure which would decrease the divergence speed and might result in an experimental value smaller than the value obtained from calculations based on a center of pressure located at the quarter chord. There is also a possibility that a gust or some change in the stability characteristics of the model due to some unknown flight conditions may have resulted in an overload on the wing.

Model 6

The wings of model 6 were similar in construction, though smaller in size, to those on model D, reported in reference 3. In the test of model D, wing failure appeared to be caused by an oscillation involving flexure of the wing and pitch of the model. In order to determine whether the position of the wings on the fuselage and the moment of inertia and mass of the fuselage basically influence this oscillation, the flight test of model 6 was conducted. For this test the leading edge of the wings was located slightly ahead of the center of gravity of the model, instead of being used as tail fins as they were on model D. The strain gages on these wings were mounted to detect bending rather than torsion.

The test results shown in figure 6(b) show that the frequency of the oscillations immediately preceding wing failure was lower than the natural first bending frequency of the wing and slightly higher than the natural pitching frequency of the model at the failure speed. This fact indicates that the flutter mode was apparently a combination of flexure of the wings and pitch of the model. In order to investigate further this type of flutter, additional tests with more complete instrumentation for detecting model pitch and translation are necessary.

Models 7, 8, 9, and 10

This group of models was tested to investigate the effect of varying the degree of sweepback on flutter speed while maintaining constant the length-to-chord ratio and the structural stiffnesses. The record of the flight of model 7 (unswept) in figure 6(c) shows erratic oscillations just before failure, but a study of this record indicates that the left-wing failure may be of the same type as the failure of the wings of model 6. The oscillations are not as smooth and the amplitude is not as large as those on the record of model 6, but it should be pointed out that this type of failure is composed primarily of wing bending and the trace on the record is that produced by torsion strain gages. If the gages happen to be placed exactly in the right position relative to each other and the wing, no bending will be detected by gages that are mounted for torsion.

Figure 6(d) shows a record of the flutter of model 8 (30° sweepback). The wings on this model fluttered at a Mach number of 0.78, corresponding to a speed of 882 feet per second. The ratios of experimental flutter speed to the reference flutter speed are 1.10 and 1.14 for the left and right wings, respectively. This difference is caused by a slight difference in the structural parameters of the wings. The experimental flutter frequency was 50 cycles per second. The calculated reference flutter frequencies are 51.2 and 48.7 cycles per second.

Model 9 (45° sweepback) and model 10 (60° sweepback) went up to the highest Mach number of the flights, 1.44 and 1.47, respectively, without flutter or failure so no reproduction of these records is shown. The ratios of the maximum experimental velocities to the reference flutter velocities for these models are 1.91 and 1.96 for model 9 (45° sweepback) and 1.50 and 1.52 for model 10 (60° sweepback) for the left and right wings, respectively. These values indicate that the theory is increasingly conservative at the higher Mach numbers. It should be pointed out that the structural parameters (table I) of models 8, 9, and 10 are quite similar. This fact leads to the conclusion that the primary reason for no flutter in the tests of the wings of models 9 and 10 was the fact that they were more highly swept than those of model 8. It might also be pointed out that since this series of wings had a constant length-to-chord

ratio, the higher sweep angles had a lower aspect ratio. Therefore, an additional aspect-ratio effect may also be involved in this series of tests.

Models 11, 12, and 13

This group of models was tested to investigate the effect of varying the degree of sweepback while maintaining the aspect ratio constant. Unfortunately, for this particular group of tests, no conclusions may be drawn concerning the effect of sweep on flutter since models 11 (unswept) and 12 (30° sweepback) diverged. The wing of model 11 failed at a Mach number of 0.97 corresponding to a speed of 1100 feet per second while the calculated divergence speed was 1028 feet per second. Although these wings did not flutter, the tests have value in that they show that the flutter region for this type of wing is above the points at which these wings failed.

Concerning model 12, as in the case of model 5, divergence does not have a definite explanation. The ratio of the experimental failure speed to the calculated divergence speed is 0.544.

A possible explanation of the failure of models 11 and 12 might be vehicle instability. Such a phenomenon has been noted when the size of the stabilizing fins approaches the size of the test wings and the fins lie in the plane of the wings. Such instability apparently occurs only over a small range of wing angle of attack near zero and is attributed to the effect of downwash on the tail surfaces. In this case failure would be caused by simple overloading of the wings and not by divergence. It may be noted that an angle of incidence of approximately 3° would create sufficient load to cause wing failure.

The flutter of model 13 is interesting in that it occurred at a Mach number of 1.01, corresponding to a speed of 1130 feet per second. The ratio of experimental flutter speed to the calculated flutter speed is 1.38 and 1.37 for the left and right wings, respectively. The experimental flutter frequency was 107 cycles per second. The reference flutter frequencies are 91.6 and 92.25 cycles per second for the left and right wings, respectively.

The calculated flutter speeds used in obtaining the ratios referred to previously are obtained from the theory of reference 5. A plot of the ratios of the various experimental velocities to the reference velocities as a function of Mach number is presented in figure 7. While sufficient data were not obtained to make any conclusive statements concerning these low-aspect-ratio wings, there is the same indication as that pointed out in reference 11 relative to straight wings; that is, that above a Mach number of approximately 0.9 and on up to the limit of

these tests the incompressible theory becomes more conservative. There is the indication, as in reference 11, that the region around $M = 0.9$ is the critical flutter region for these low-aspect-ratio ($A < 4$) wings with length-to-chord ratios of 3. These data are supplemented by some unpublished results obtained from tests run in the Langley supersonic flutter apparatus ($M = 1.3$), where all wings that fluttered in supersonic flow, with the exception of 60° sweptback wings with length-to-chord ratios of 5 or higher, also fluttered when subjected to subsonic flow. Further investigation with wings of higher aspect ratios is necessary to enlarge upon the results that have been obtained.

It should be emphasized that the calculated flutter speeds are based on a theory which employs two-dimensional incompressible flow and are not expected to agree with experiments in the Mach number range of these tests. However, these calculations may be used as a standard with which the data of this and other test programs may be compared. When sufficient experimental data have been obtained, it may serve as a convenient design criterion which could be used in lieu of a more exact method of calculating transonic flutter speeds.

CONCLUDING STATEMENTS

Wings of various aspect ratios and amounts of sweepback have been tested using rocket-propelled vehicles. The first pair tested diverged and failed at a speed that was 200 feet per second less than the lowest value calculated from various divergence theories. The second pair tested failed in a low-frequency flutter mode which was apparently a combination of wing bending and body pitch.

Tests of one series of wings of constant length-to-chord ratios and stiffnesses and varying sweepback angles resulted in an unswept wing failing apparently in the same low-frequency flutter mentioned previously. The 30° sweptback wings of this series fluttered at a Mach number of 0.78 in a wing bending-torsion flutter mode. The experimental speed exceeds the flutter speed calculated by use of the incompressible swept-wing theory of NACA RM L8H30 by about 12 percent. Similar wings with 45° and 60° sweepback did not flutter up to the highest Mach number of the tests (1.44 and 1.47, respectively). The maximum experimental speeds attained exceed the calculated speeds by about 93 percent in the case of the 45° sweptback wings and by about 50 percent in the case of the 60° sweptback wings.

In another series of tests on wings of constant aspect ratio the unswept and 30° sweptback wings diverged and the 60° sweptback wings

fluttered at a Mach number of 1.01. The experimental flutter speed exceeded the calculated reference flutter speed by about 37 percent.

Langley Aeronautical Laboratory
National Advisory Committee for Aeronautics
Langley Air Force Base, Va.

REFERENCES

1. Angle, Ellwyn E.: Initial Flight Test of the NACA FR-1-A, a Low-Acceleration Rocket-Propelled Vehicle for Transonic Flutter Research. NACA RM L7J08, 1948.

2. Angle, Ellwyn E., Clevenson, Sherman A., and Lundstrom, Reginald R.: Flight Test of NACA FR-1-B, a Low-Acceleration Rocket-Propelled Vehicle for Transonic Flutter Research. NACA RM L8C24, 1948.

3. Lundstrom, Reginald R., Lauten, William T., Jr., and Angle, Ellwyn E.: Transonic-Flutter Investigation of Wings Attached to Two Low-Acceleration Rocket-Propelled Vehicles. NACA RM L8I30, 1948.

4. Barmby, J. G., and Teitelbaum, J. M:: Initial Flight Tests of the NACA FR-2, a High-Velocity Rocket-Propelled Vehicle for Transonic Flutter Research. NACA RM L7J20, 1948.

5. Barmby, J. G., Cunningham, H. J., and Garrick, I. E.: Investigation of the Effect of Sweep on the Flutter of Cantilever Wings. NACA RM L8H30, 1948.

6. Diederich, Franklin W., and Budiansky, Bernard: Divergence of Swept Wings. NACA TN 1680, 1948.

7. Tuovila, W. J., Baker, John E., and Regier, Arthur A.: Initial Experiments on Flutter of Unswept Cantilever Wings at Mach Number 1.3. NACA RM L8J11, 1949.

8. Theodorsen, Theodore, and Garrick, I. E.: Mechanism of Flutter - A Theoretical and Experimental Investigation of the Flutter Problem. NACA Rep. 685, 1940.

9. Barmby, J. G., and Clevenson, S. A.: Initial Test in the Transonic Range of Four Flutter Airfoils Attached to a Freely Falling Body. NACA RM L7B27, 1947.

10. Clevenson, S. A., and Lauten, William T., Jr.: Flutter Investigation in the Transonic Range of Six Airfoils Attached to Three Freely Falling Bodies. NACA RM L7K17, 1948.

11. Lauten, William T., Jr., and Barmby, J. G.: Continuation of Wing Flutter Investigation in the Transonic Range and Presentation of a Limited Summary of Flutter Data. NACA RM L9B25b, 1949.

TABLE I

WING PARAMETERS

Wing	c.g.	L.E.	Section	M_{cr}	c (in.)	l (in.)	A	A_g	b	x_1	x_o	a	a + x_α	$1/\kappa$(stnd.)	r_α^2	f_{h_1}	f_{h_2}	f_t	f_α	g_h	g_α	GJ	EI	Λ
FR2-5L	42	40	9 percent thick circular arc	0.82	8	24	7.32	3	0.3333	68.8	63.3	0.266	0.375	101.2	0.2485	22.5	-----	138.5	130.6	0.02	0.04	364×10^3	447×10^3	0
FR2-5R	42	40	9 percent thick circular arc	.82	8	24	7.32	3	.3333	68.7	67.2	.344	.374	98.8	.234	24	-----	142	141.8	.02	.04	381.7	468	0
FR2-6L	41	40	NACA 65A006	.84	8	24	7.32	3	.3333	42.2	36.7	-.266	-.156	30.4	.1762	20.5	122	138.5	133.5	.02	.02	79.8	82.1	0
FR2-6R	41	40	NACA 65A006	.84	8	24	7.32	3	.3333	42.6	37.1	-.258	-.146	30.5	.1825	20.5	126	142.5	137.4	.02	.02	81.9	78.25	0
FR2-7L	41.5	40	NACA 65A009	.79	8	24	7.32	3	.3333	44.5	39.1	-.218	-.108	42.6	.2314	28.5	171	111	108	.03	.03	80.0	214.2	0
FR2-7R	41.5	40	NACA 65A009	.79	8	24	7.32	3	.3333	45.3	40.6	-.186	-.094	41.7	.2324	26.5	162	108	105.8	.03	.03	75.3	193	0
FR2-8L	40.8	32	NACA 65A009	.79	8	24	5.64	2.25	.3333	45.4	53.9	.078	-.094	40.8	.2463	26.5	166	112	104.7	.03	.03	74.4	205	30
FR2-8R	40.8	32	NACA 65A009	.79	8	24	5.64	2.25	.3333	45	61	.219	-.10	39.8	.3121	25	163.5	109	89.4	.03	.03	74.2	205	30
FR2-9L	41.2	29.7	NACA 65A009	.79	8	24	3.93	1.49	.3333	45.3	68.75	.375	-.094	40.2	.4471	30.1	-----	114	78.1	.03	.03	85.1	229	45
FR2-9R	41.2	29.7	NACA 65A009	.79	8	24	3.93	1.49	.3333	45.3	70.31	.406	-.094	39.1	.4775	29.8	-----	110	72.6	.03	.03	86.9	210.5	45
FR2-10L	41.2	27.8	NACA 65A009	.79	8	24	2.16	.75	.3333	44.5	68.75	.375	-.108	41.6	.4581	36	190	111.5	73.3	.03	.03	87.1	184	60
FR2-10R	41.2	27.8	NACA 65A009	.79	8	24	2.16	.75	.3333	45.3	71.88	.4375	-.094	41.2	.505	35.5	188	111	68.2	.03	.03	86.5	176.6	60
FR2-11L	41.2	40	NACA 65A005	.86	8	8	3.31	1	.3333	44.5	43.75	-.125	-.109	16.7	.2173	134	-----	199.5	199.25	.03	.03	14.39	25.25	0
FR2-11R	41.2	40	NACA 65A005	.86	8	8	3.31	1	.3333	45.3	43.0	-.142	-.094	18.6	.2392	151.5	-----	224	222	.03	.03	18.7	36.5	0
FR2-12L	41.2	35.9	NACA 65A005.8	.845	6.93	9.23	3.31	1	.2889	44.5	55.89	.1174	-.1104	18.8	.2837	105.5	-----	196.5	169.2	.03	.03	14.62	37	30
FR2-12R	41.2	35.9	NACA 65A005.8	.845	6.93	9.23	3.31	1	.2889	44.5	54.5	.09	-.1104	17.8	.2651	110.5	-----	201.0	177.5	.03	.03	11.62	26.98	30
FR2-13L	41.2	31	NACA $65A_{(06)}010$	.76	4	16	3.31	1	.1667	45.3	65.62	.312	-.094	29.9	.39	49	-----	181.5	133.7	.03	.03	4.88	13.39	60
FR2-13R	41.2	31	NACA $65A_{(06)}010$	.76	4	16	3.31	1	.1667	45.3	67.25	.345	-.094	28.8	.4172	49	-----	187	132.7	.03	.03	4.808	12.86	60

NACA

TABLE II

EXPERIMENTAL AND CALCULATED RESULTS

Wing	M_e	v_e	f_{f_e}	v_m	ρ	q	$\frac{1}{\kappa}$	T	v_c	p_s	v_R	f_R	v_D	$\frac{v_R \cos \Lambda}{b\omega_\alpha}$	$\frac{1}{k}$	$\frac{v_e}{v_R}$	$\frac{v_m}{v_R}$
FR2-5L	0.82	----	---	912	0.2428×10^{-2}	1009.7	99.25	510.5	1111	2123	1029.8	44.7	1127	3.765	11.0	-----	0.886
FR2-5R	-----	----	---	----	.2428	------	98.81	510.5	1111	2123	1095.9	47.6	1244	3.69	11.0	-----	-----
FR2-6L	.75	----	---	836	.2408	841.5	30.03	518	1115.4	2138	789.9	59.6	958	2.825	6.33	-----	1.058
FR2-6R	-----	----	---	----	.2408	------	30.12	518	1115.4	2138	814.4	61.6	955	2.83	6.31	-----	-----
FR2-7L	.79	----	---	875	.2445	936	41.49	511.5	1112	2141	752.1	54.7	827	3.325	6.56	-----	1.164
FR2-7R	-----	----	---	----	.2445	------	40.59	511.5	1112	2141	725.7	52.6	762	3.275	6.565	-----	-----
FR2-8L	.784	882	50	----	.2355	916	41.24	525.6	1127	2120	805.2	51.2	∞	3.18	6.5	1.095	-----
FR2-8R	.784	882	50	----	.2355	916	40.27	525.6	1127	2120	775.1	48.7	∞	3.585	6.579	1.138	-----
FR2-9L	1.44	----	---	1640	.2335	3140	40.85	533.3	1137	2132	872.1	54.1	∞	3.77	5.44	-----	1.88
FR2-9R	1.44	----	---	1640	.2335	3140	39.71	533.3	1137	2132	845.1	52.7	∞	3.93	5.41	-----	1.94
FR2-10L	1.47	----	---	1670	.233	3249	42.46	530.5	1134	2120	1114.5	56.1	$-q^a$	3.63	4.74	-----	1.498
FR2-10R	1.47	----	---	1670	.233	3249	42.02	530.5	1134	2120	1097.3	54.3	$-q^a$	3.84	4.825	-----	1.521
FR2-11L	.97	----	---	1100	.2288	1384	17.38	537.6	1136	2109	834.6	152.7	1028	2.00	2.61	-----	1.317
FR2-11R	-----	-----	---	----	.2288	------	19.38	537.6	1136	2109	871.8	176.0	1200	1.875	2.365	-----	-----
FR2-12L	-----	----	---	----	.2289	------	19.61	536.6	1135	2108	922.4	135.4	1407	2.6	3.25	-----	-----
FR2-12R	.81	----	---	920	.2289	968.7	18.55	536.6	1135	2108	915.5	144.1	1690	2.46	3.03	-----	1.005
FR2-13L	1.01	1130	107	----	.2352	1502	30.24	522.5	1120	2113	816.5	91.6	∞	2.915	4.26	1.384	-----
FR2-13R	1.01	1130	107	----	.2352	1502	29.15	522.5	1120	2113	822.5	92.25	∞	2.96	4.25	1.374	-----

[a]See equations (1) and (2) of reference 3.

Page intentionally left blank

Page intentionally left blank

NACA
L-60920

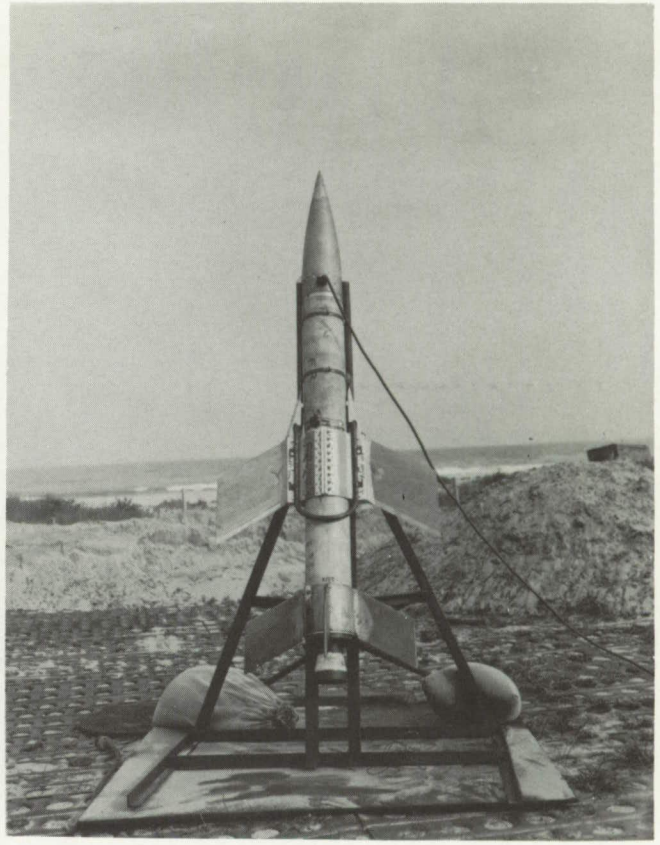

NACA
L-61651

Figure 1.- Photographs of representative models on the launching rack.

Page intentionally left blank

Page intentionally left blank

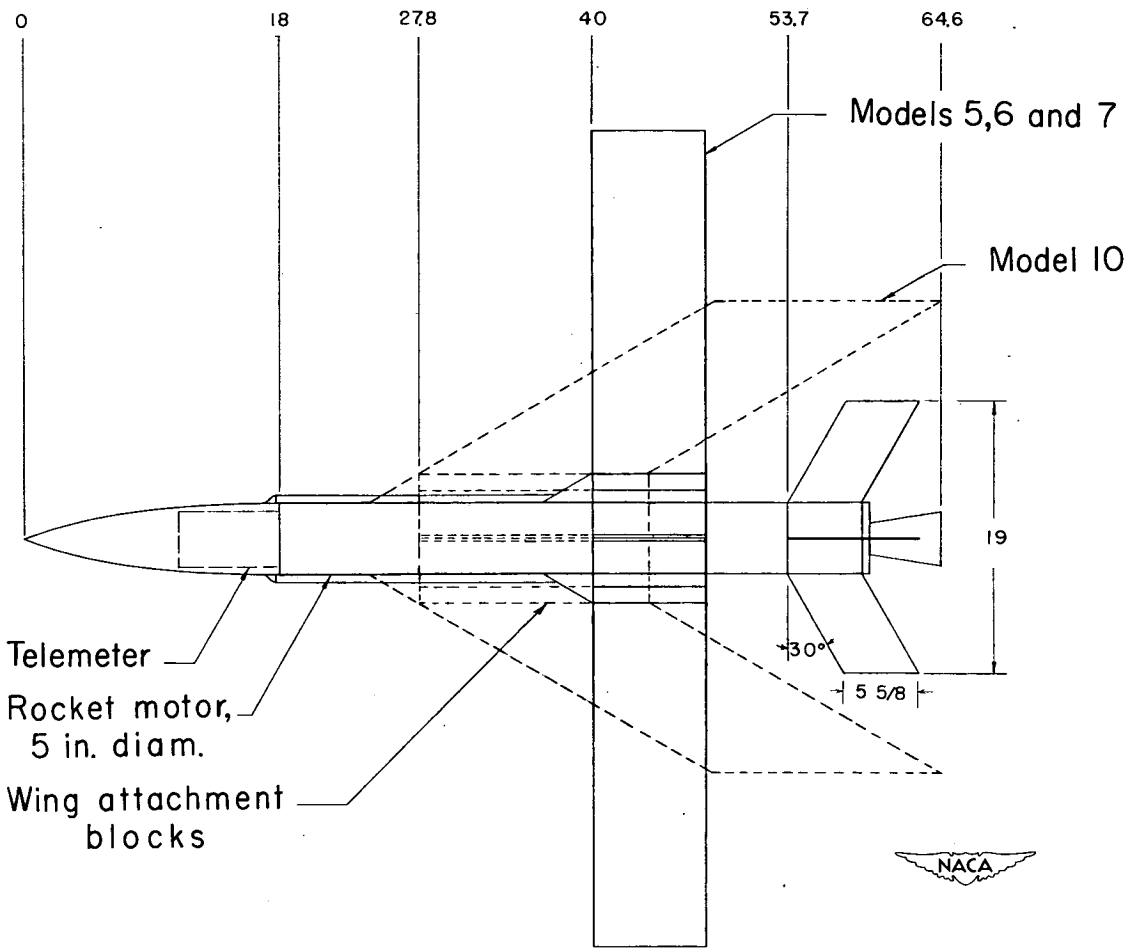

Figure 2.- Sketch of test vehicle showing attachment of an unswept and a 60° sweptback wing. (All dimensions are in inches.)

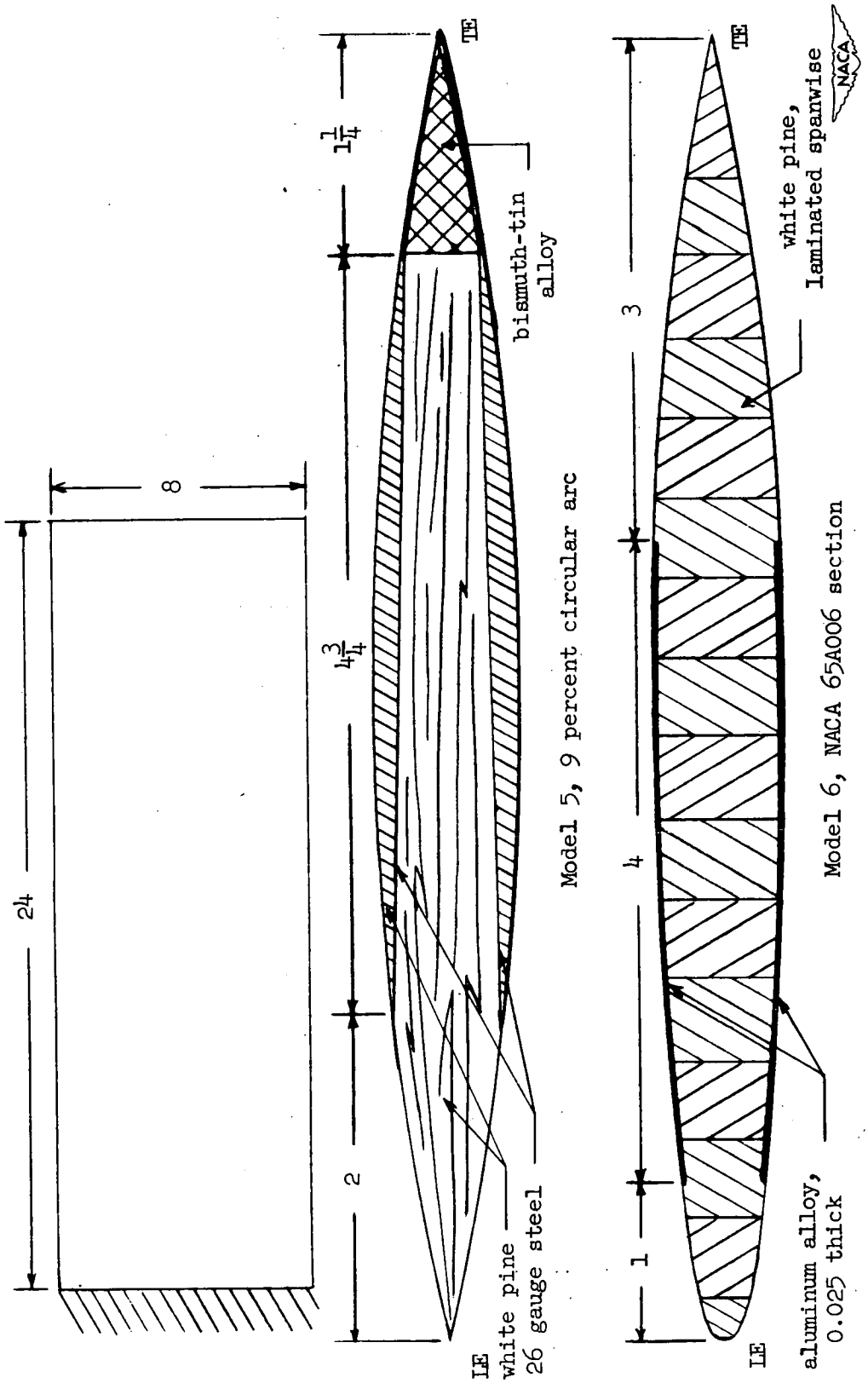

Figure 3.- Sketch of wings of models 5 and 6. (All dimensions are in inches.)

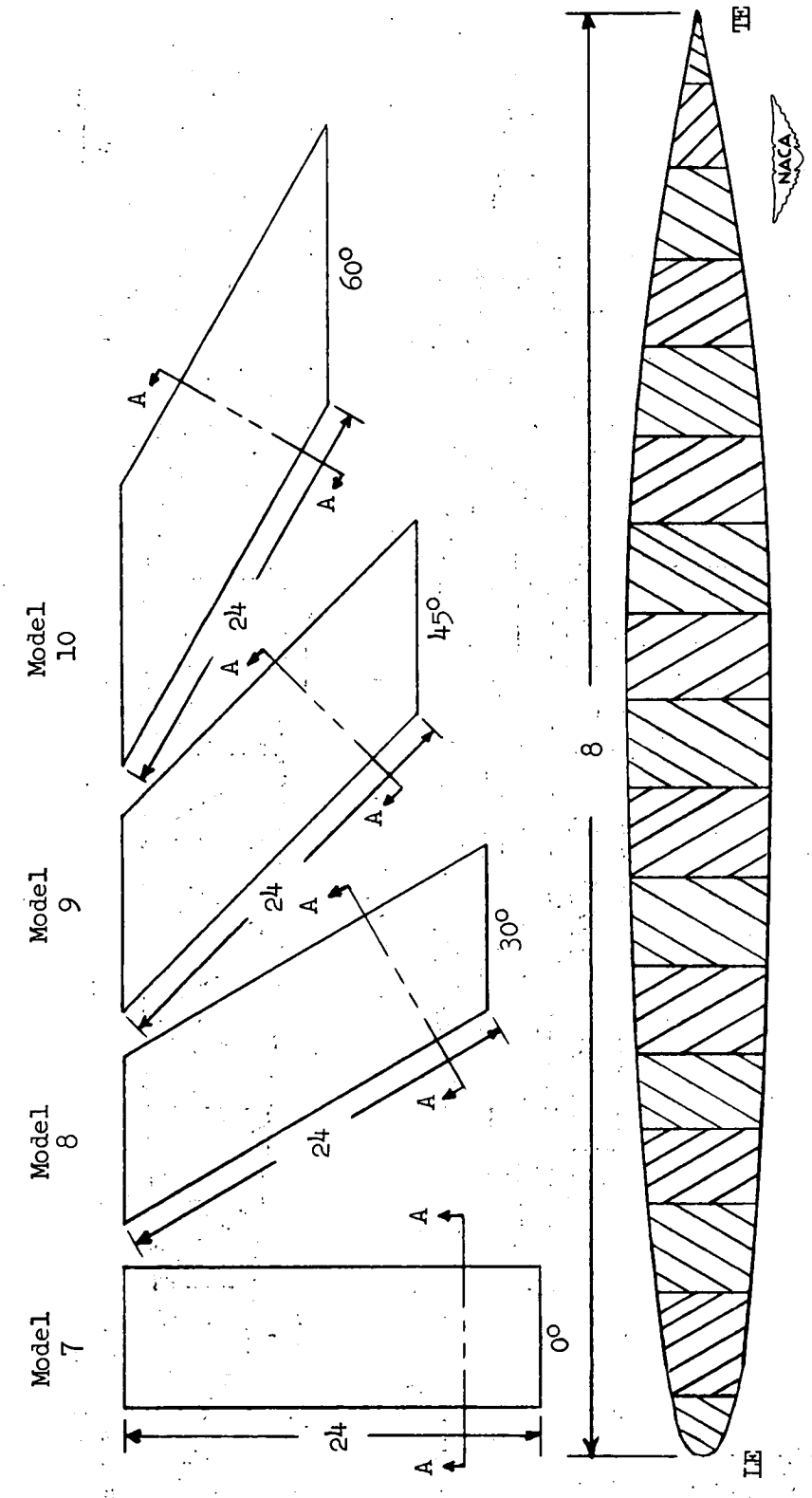

Section AA, NACA 65A009, laminated maple

Figure 4.- Sketch of wings of models 7, 8, 9, and 10. (All dimensions are in inches.)

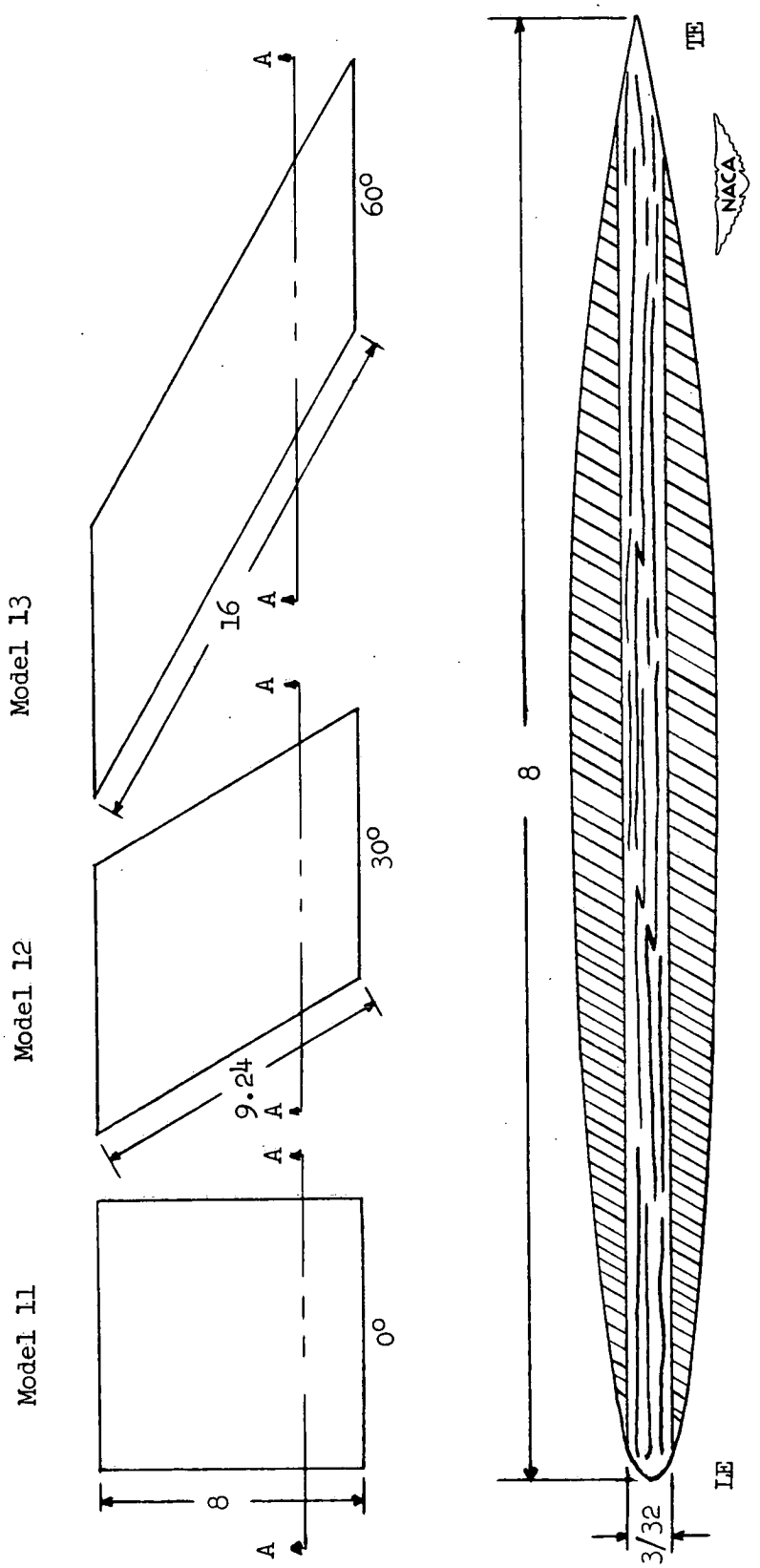

Figure 5.- Sketch of wings of models 11, 12, and 13. (All dimensions are in inches.)

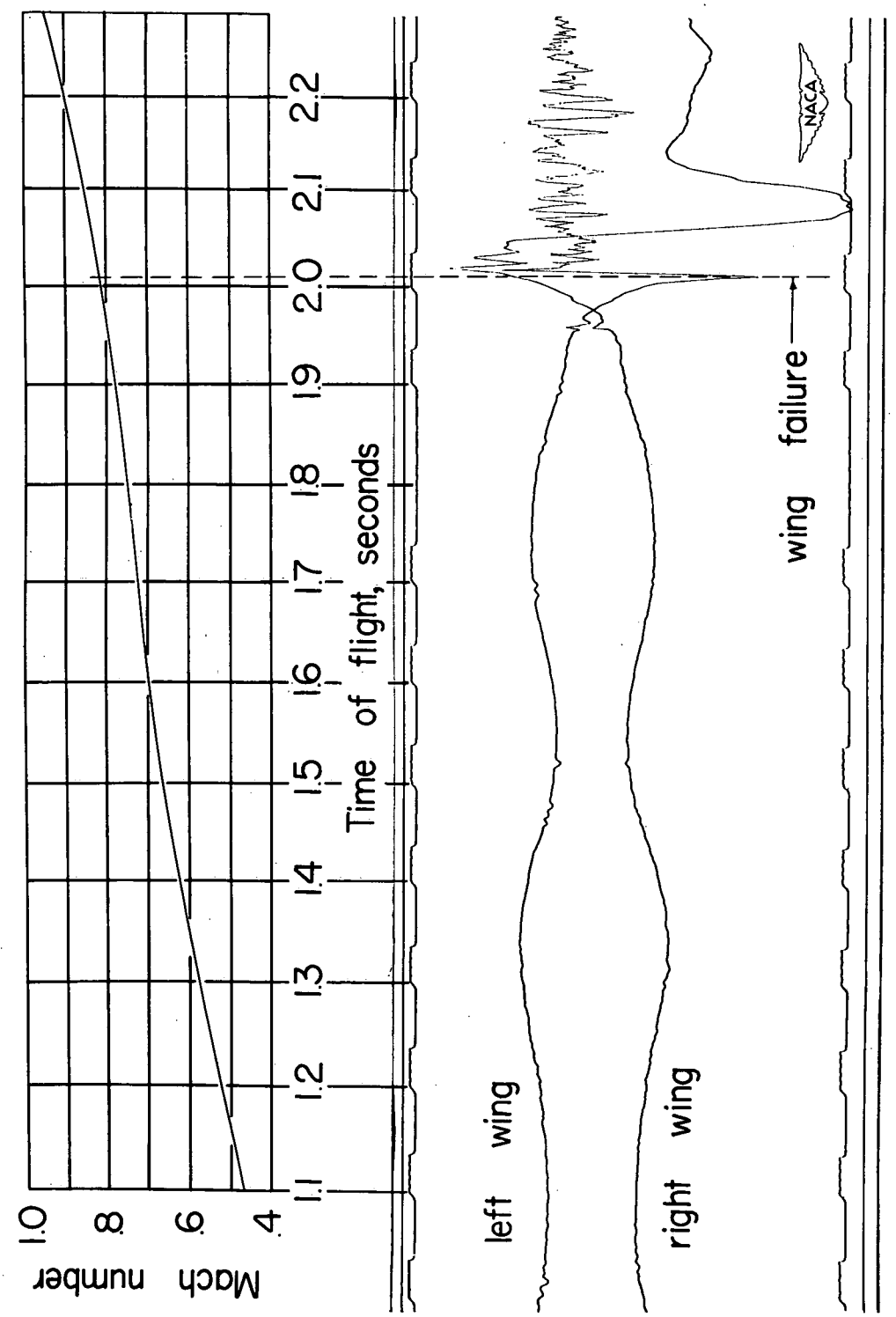

(a) Model 5; A = 7.3; $\Lambda = 0^{\circ}$; v_c = 1111 feet per second.

Figure 6.- Portions of telemeter records obtained during the flight tests with Mach number plots added.

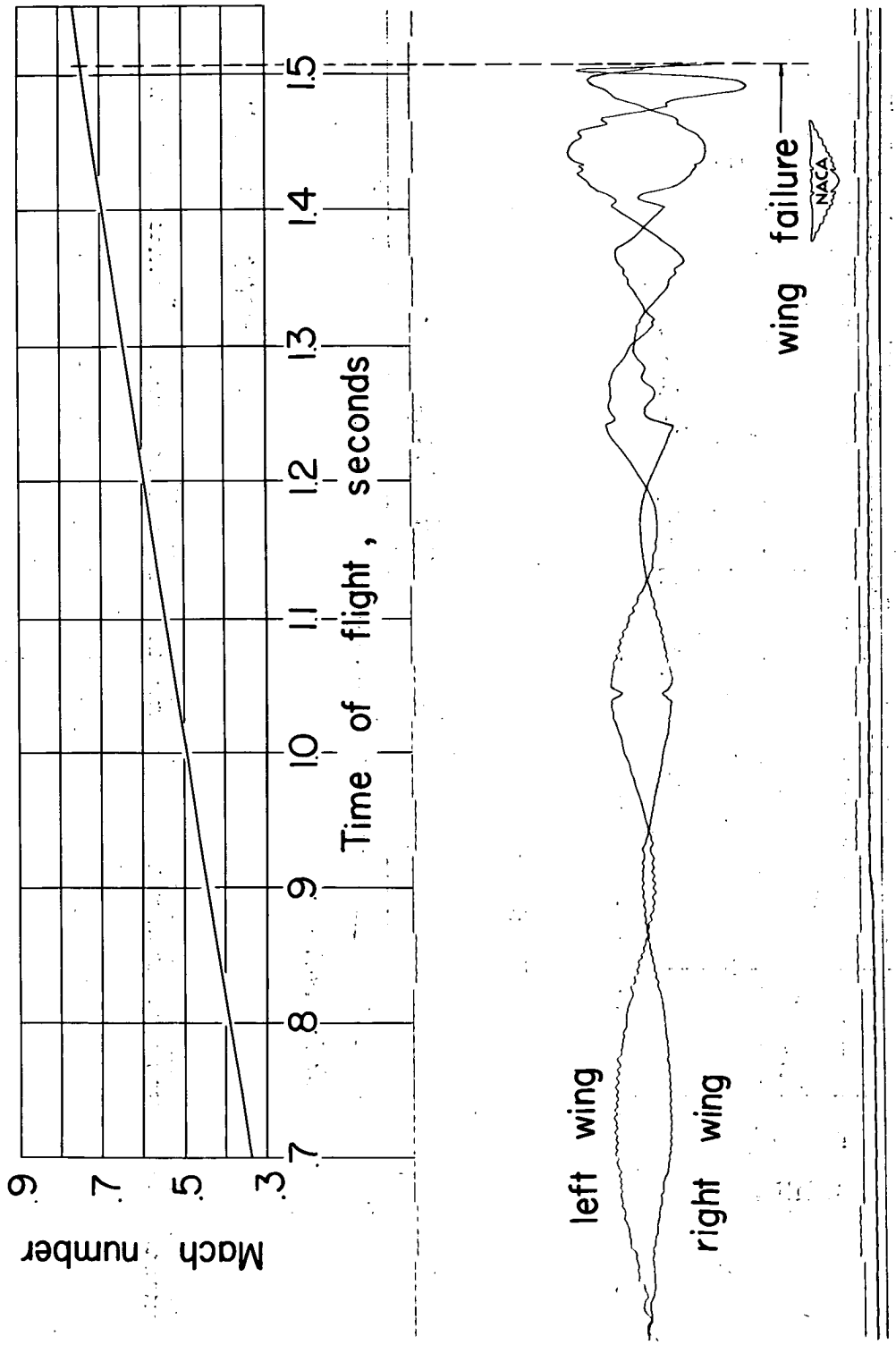

(b) Model 6; $A = 7.3$; $\Lambda = 0^{\circ}$; $V_c = 1115.4$ feet per second.

Figure 6.- Continued.

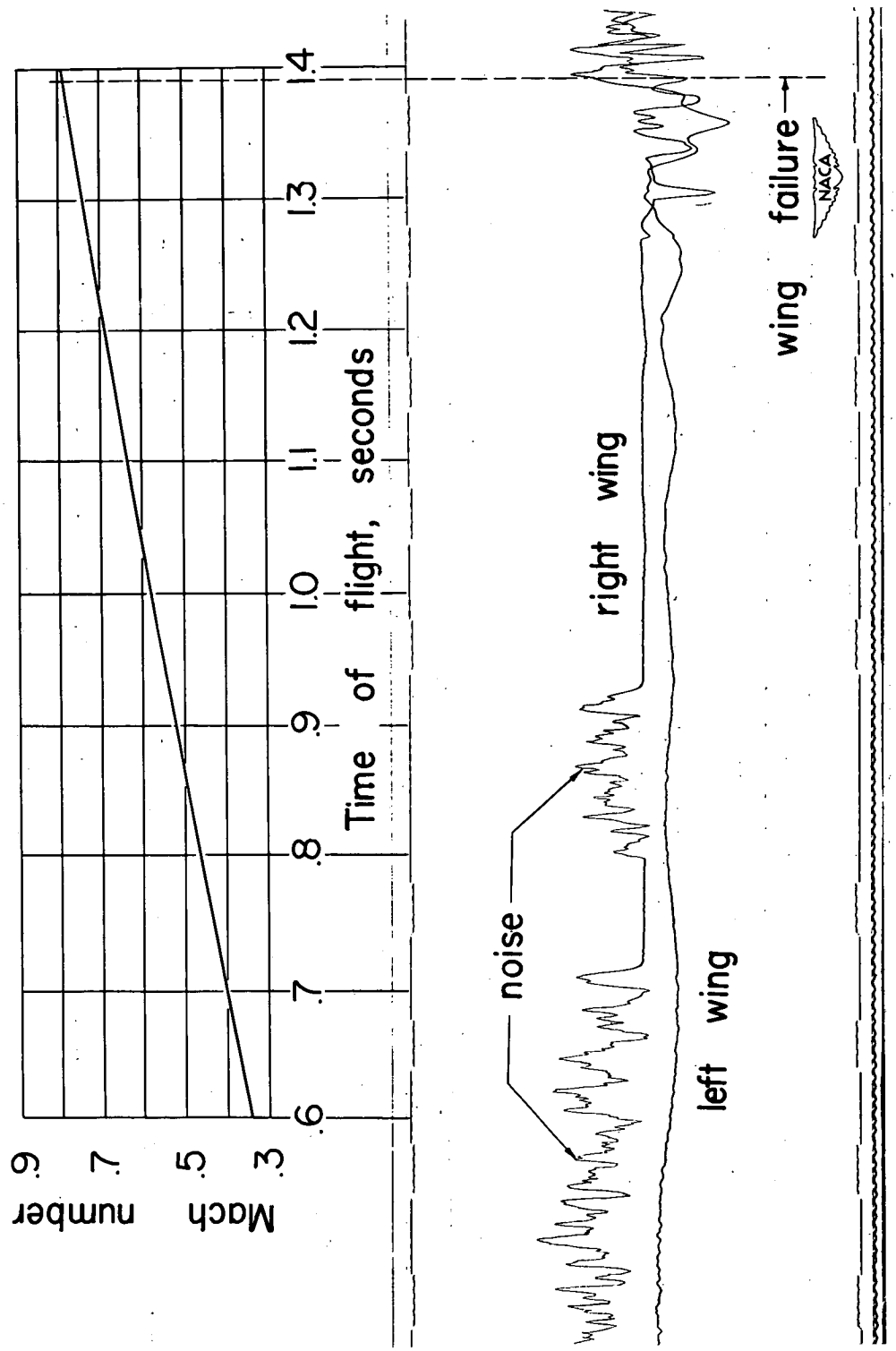

(c) Model 7; $A = 7.3$; $\Lambda = 0^{\circ}$; $V_c = 1112$ feet per second.

Figure 6.- Continued.

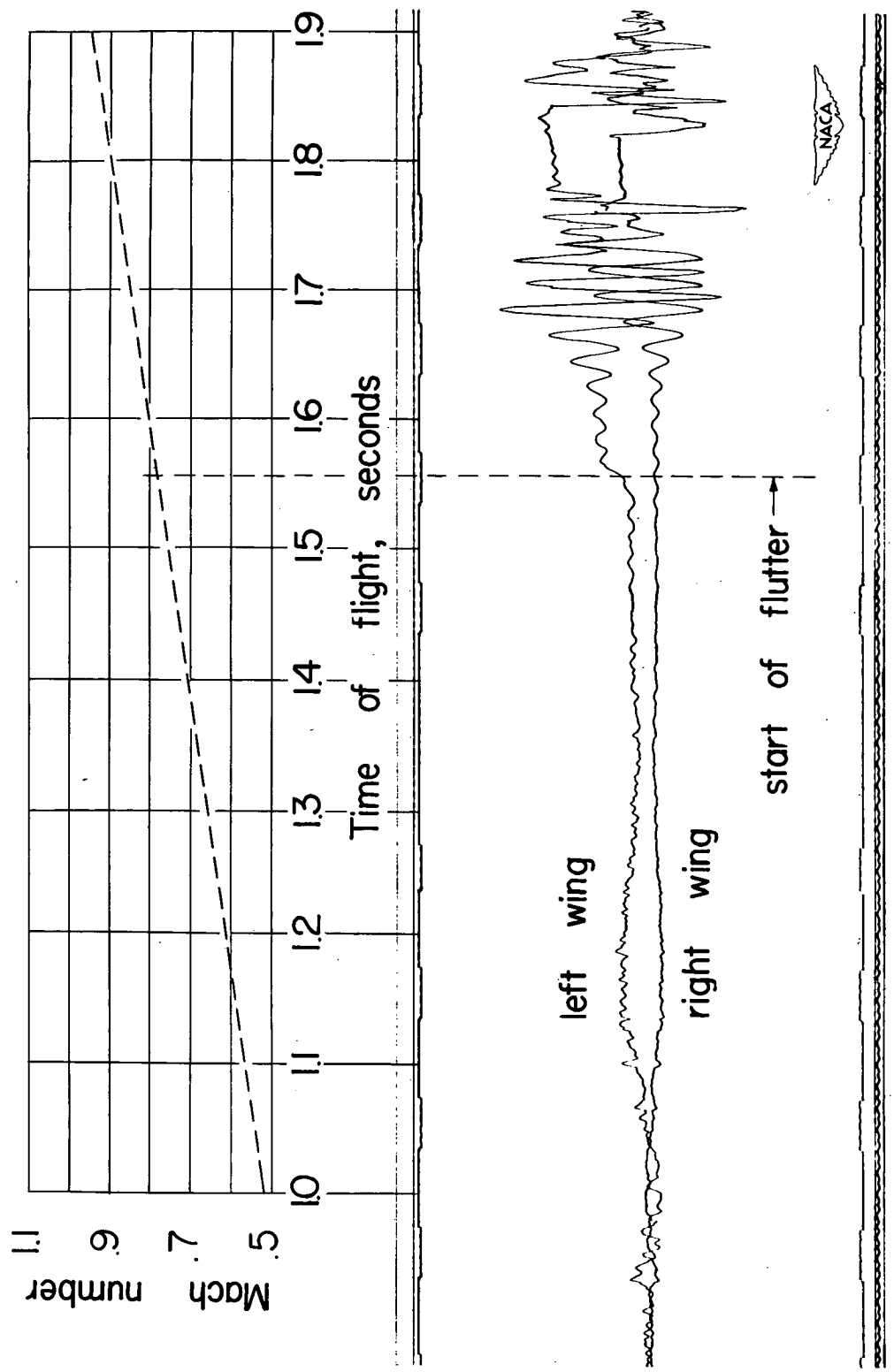

(d) Model 8; $A = 5.6$; $\Lambda = 30°$; $V_c = 1127$ feet per second.

Figure 6.- Continued.

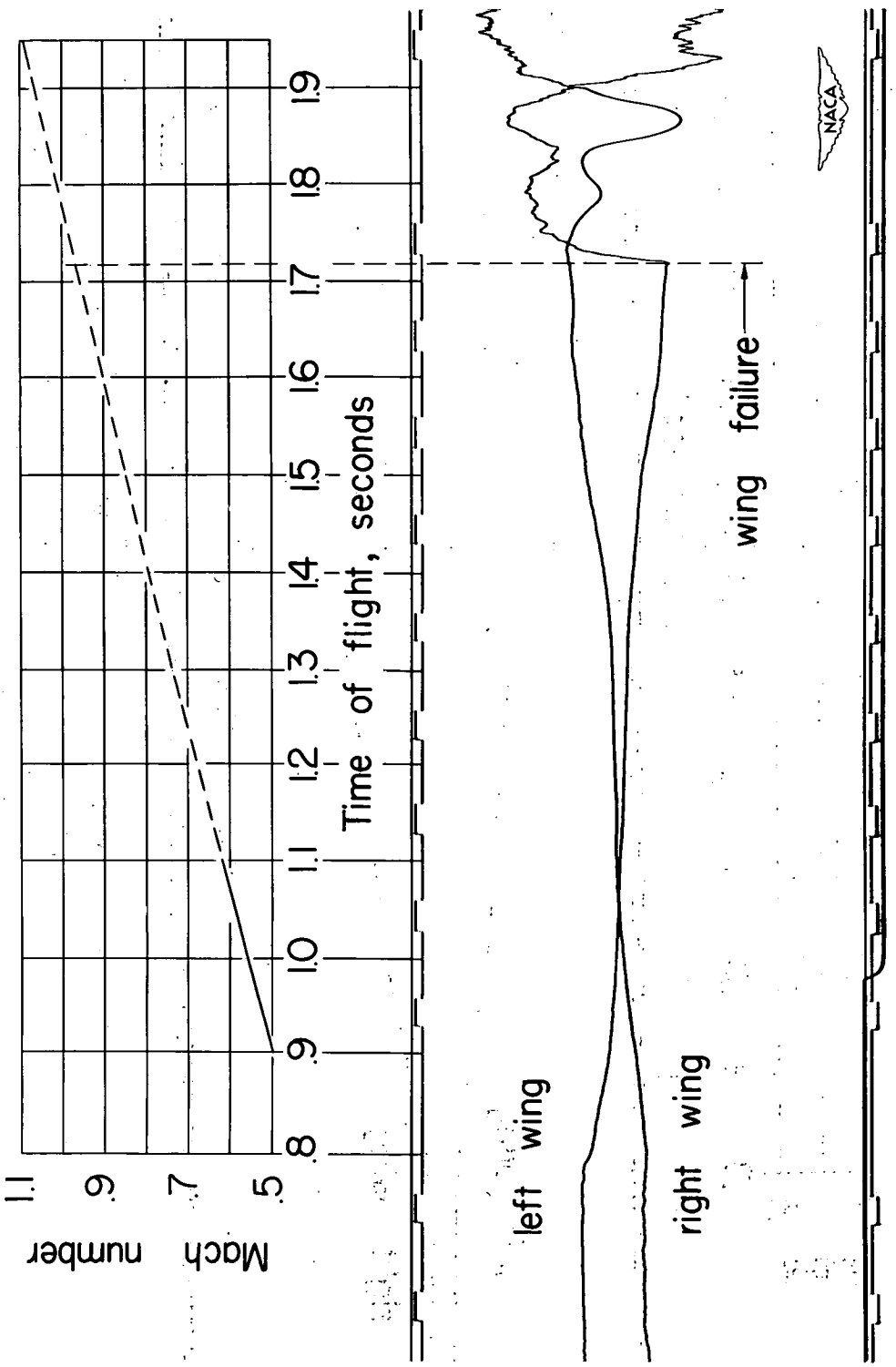

(e) Model 11; A = 3.3; $\Lambda = 0^{\circ}$; v_c = 1136 feet per second.

Figure 6.- Continued.

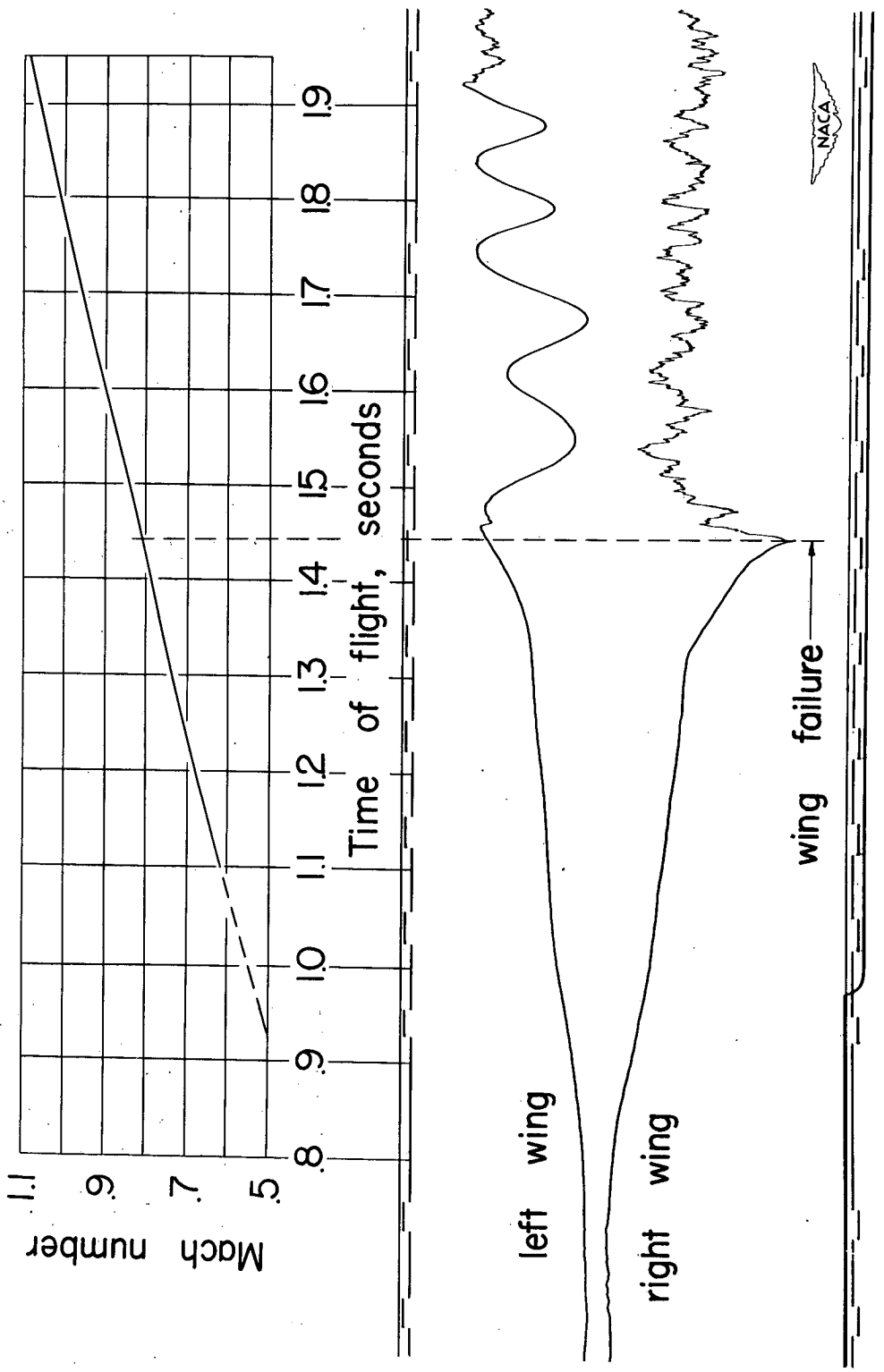

(f) Model 12; $A = 3.3$; $\Lambda = 30^{\circ}$; $v_c = 1135$ feet per second.

Figure 6.- Continued.

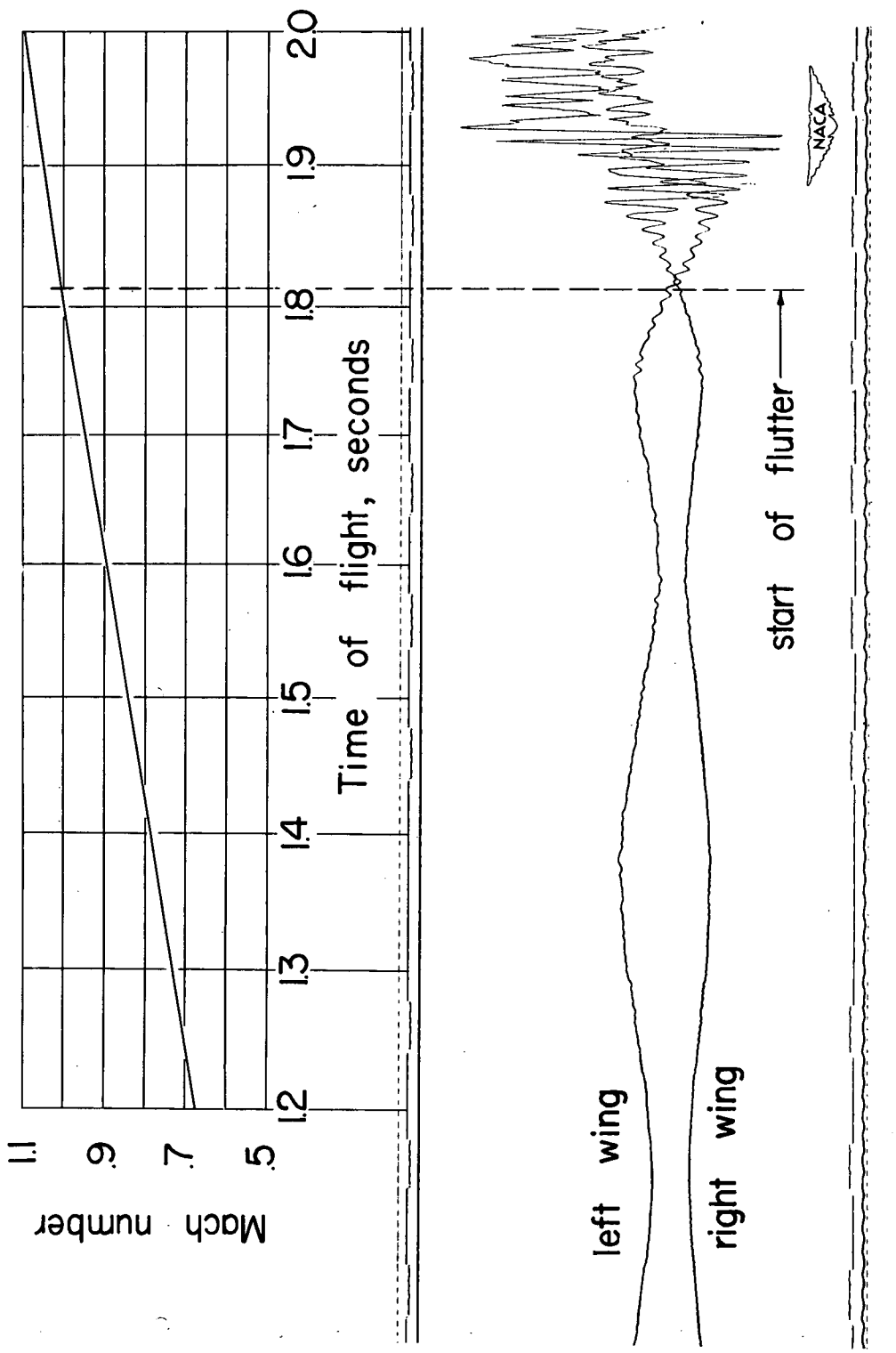

(g) Model 13; $A = 3.3$; $\Lambda = 60°$; $V_c = 1120$ feet per second.

Figure 6.- Concluded.

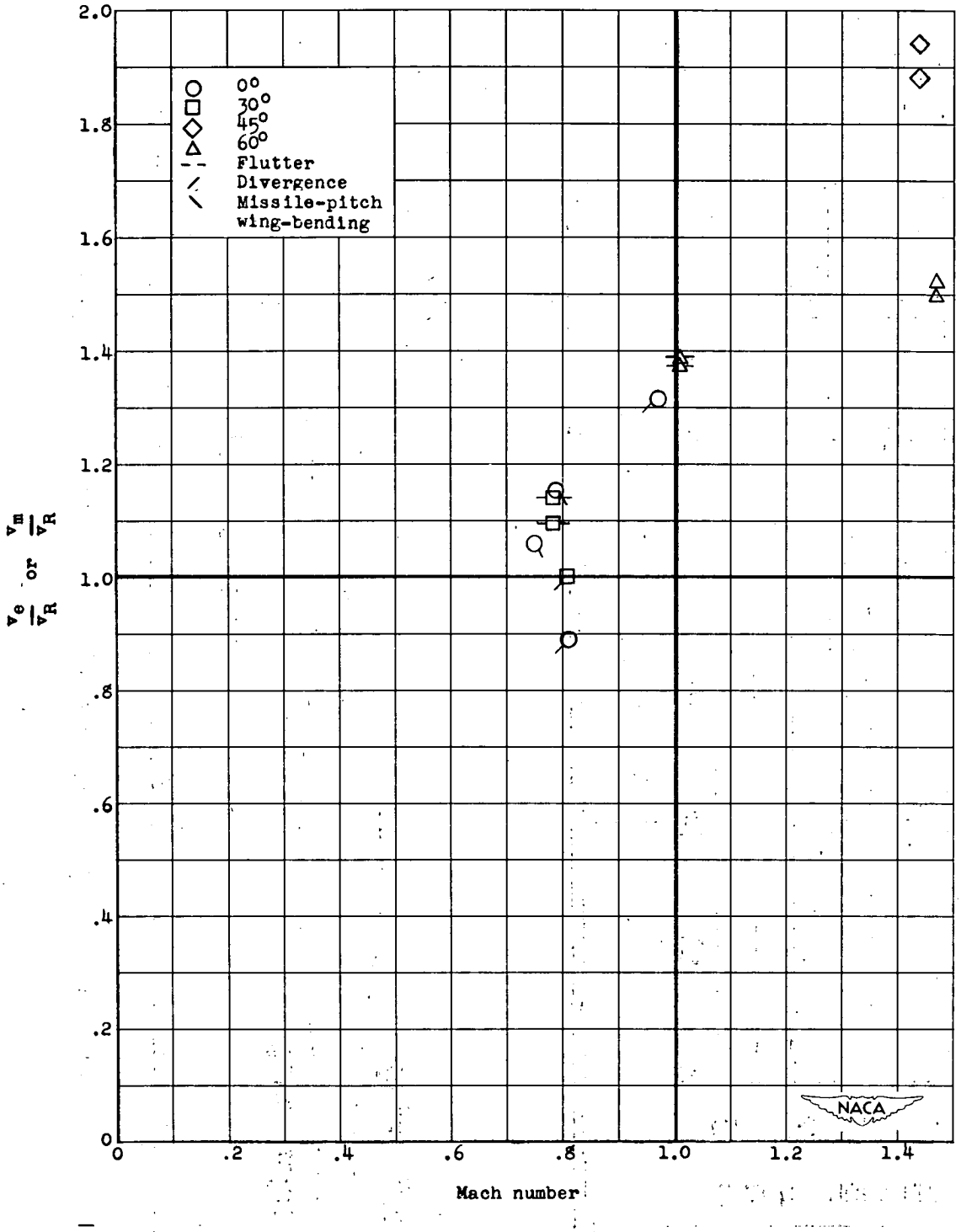

Figure 7.- Plot of $\frac{v_e}{v_R}$ and $\frac{v_m}{v_R}$ against Mach number.